Rock Mechanics and Rock Engineering (2018) 51:3179–3188
https://doi.org/10.1007/s00603-018-1530-1

TECHNICAL NOTE

Re-examination of the In Situ Stress Measurements on the 240 Level of the AECL's URL Using Tensor-Based Approaches

Ke Gao[1,2] · **John P. Harrison**[1]

Received: 18 March 2018 / Accepted: 16 June 2018 / Published online: 28 June 2018

Keywords In situ stress · Euclidean mean · Effective variance · Stress variability · Stress measurement

1 Introduction

In situ stress is an important parameter in rock mechanics and often displays significant variability in fractured rock masses (Day-Lewis 2008; Hyett 1990; Martin 1990; Matsumoto et al. 2015; Obara and Sugawara 2003). Therefore, rigorous statistical approaches for stress variability characterisation are essential components and prerequisites for adequate interpretation of stress measurements. However, currently in rock mechanics, stresses are customarily processed by analysing the principal stress magnitude and orientation separately (e.g. Brown and Hoek 1978; Hakami 2011; Hast 1969; Herget 1988; Lisle 1989; Zhao et al. 2013). As previous works show, these customary scalar/vector approaches violate the tensorial nature of stress and may yield erroneous results (Dyke et al. 1987; Gao 2017; Gao and Harrison 2016b, 2017, 2018b, c; Hudson and Cooling 1988; Hudson and Harrison 1997).

Since stress is a second-order tensor, it has been advocated by many researchers that stress should be processed based on stress tensors referred to a common Cartesian coordinate system (Dyke et al. 1987; Dzik et al. 1989; Hudson and Cooling 1988; Hyett et al. 1986; Jupe 1994; Koptev et al. 2013; Martin et al. 1990; Martin and Simmons 1993; Walker et al. 1990). By considering the tensorial nature of stress, we have proposed a series of tensor-based approaches, such as Euclidean mean (a mean stress calculation approach) (Gao and Harrison 2016b, 2018a) and effective variance (a scalar-valued measure of overall stress variability) (Gao and Harrison 2016a, 2018c; Gao and Lei 2018), for stress variability characterisation. In the present paper, using these recently developed tensor-based approaches, the in situ stresses measured at the Atomic Energy of Canada Limited (AECL)'s Underground Research Laboratory (URL) in south-eastern Manitoba of Canada (Martin and Christiansson 1991b) are re-examined to provide, for the first time, a fully quantitative interpretation of stress measurement data to confirm and enhance the qualitative conclusions drawn by the original authors and give an example of how the tensor-based approaches may assist in stress data elucidation.

In the following sections, the background of the in situ stress measurements, the Euclidean mean of the measured in situ stresses and its comparison with the scalar/vector mean, as well as their effective variance are calculated and presented. Conclusions are given regarding the applicability and efficacy of the tensor-based approaches for stress variability characterisation. The definitions of Euclidean mean, scalar/vector mean and effective variance are shown in the Appendices.

2 Background of the In Situ Stress Measurements

To investigate how in situ stresses are distributed in a relatively uniform, massive granite rock mass, Martin and Christiansson (1991a) conducted 101 overcore in situ stress tests using the CSIR triaxial strain cell (Martin and Christiansson 1991b) on the 240 Level of the AECL's URL (Fig. 1), where geomechanics research was conducted during the period of about 1982–2004 to assess the feasibility of deep disposal of nuclear fuel waste in a plutonic rock mass (Chandler 2003; Martin 1990). The granite in the whole testing area is essentially unfractured except for a single fracture—the Room 209 Fracture, which strikes about 040°/220°, dips

✉ Ke Gao
k.gao@mail.utoronto.ca

[1] Department of Civil Engineering, University of Toronto, Toronto, Canada

[2] Geophysics, Los Alamos National Laboratory, Los Alamos, USA

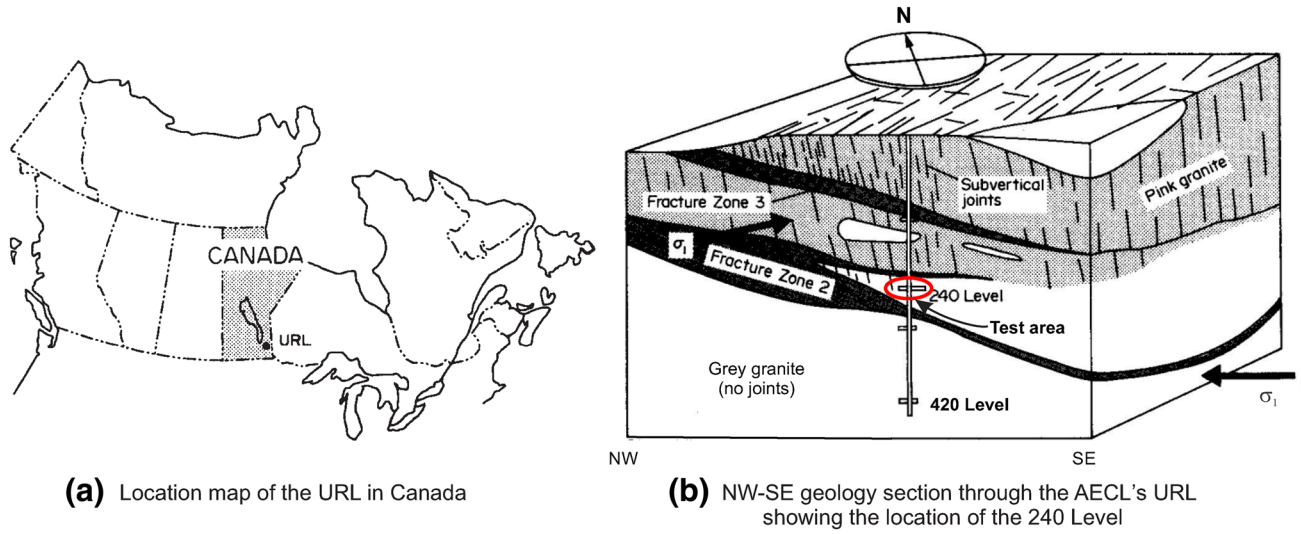

Fig. 1 Location of the AECL's URL and the position of the 240 Level (after Martin and Simmons 1993)

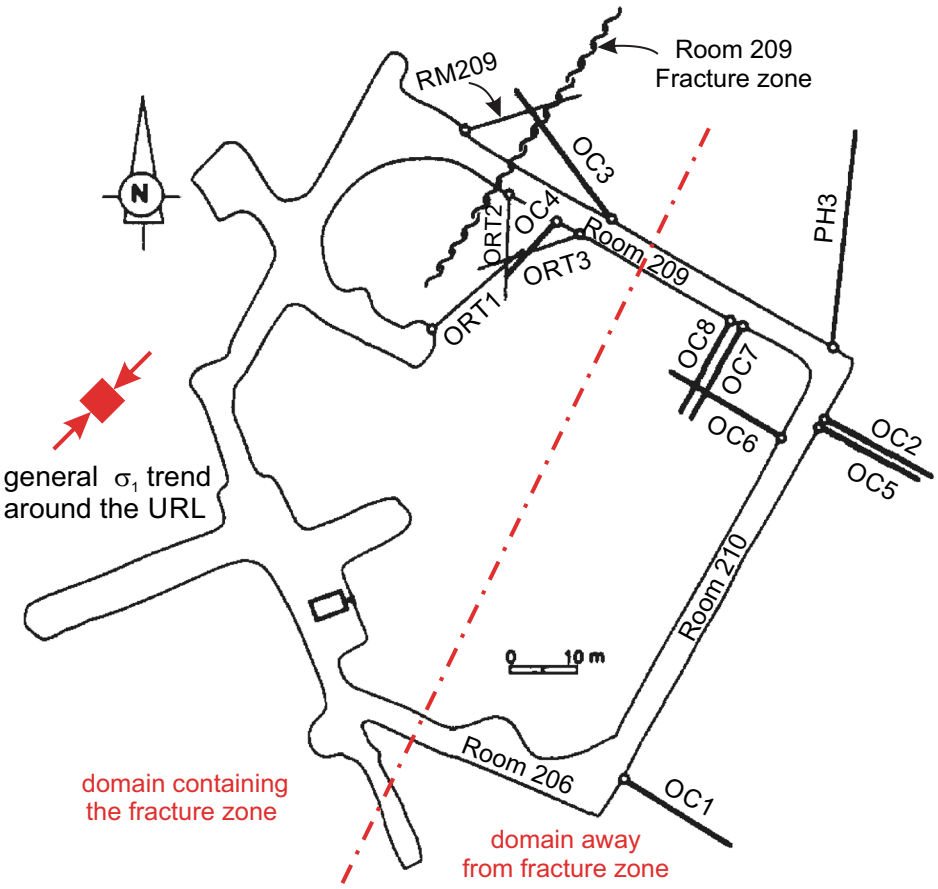

Fig. 2 Plan view of the 240 Level of the AECL's URL showing borehole locations of overcore testing (after Martin and Christiansson 1991a)

sub-vertically, and contains several short, subparallel joints that form a "fracture zone" up to 0.4 m wide (Martin and Christiansson 1991a) (Fig. 2). The tests were performed in 13 boreholes located in an area about 60 m × 60 m in plan view (Fig. 2). These tests can be deemed as being conducted within a relatively small space and time range, and spatial and temporal variabilities of the stress data were not

Table 1 Scalar/vector and Euclidean means of all in situ stress data interpreted using the isotropic model, presented in terms of principal stress magnitude and orientation

Mean	σ_1			σ_2			σ_3		
	σ_1 (MPa)	Trend (°)	Plunge (°)	σ_2 (MPa)	Trend (°)	Plunge (°)	σ_3 (MPa)	Trend (°)	Plunge (°)
Customary mean	32.5	243	27	18.4	139	52	12.2	024	67
Euclidean mean	29.3	249	18	19.4	154	16	14.3	025	65

Table 2 Scalar/vector and Euclidean means of all in situ stress data reinterpreted using the anisotropic model, presented in terms of principal stress magnitudes and orientations

Mean	σ_1			σ_2			σ_3		
	σ_1 (MPa)	Trend (°)	Plunge (°)	σ_2 (MPa)	Trend (°)	Plunge (°)	σ_3 (MPa)	Trend (°)	Plunge (°)
Customary mean	29.4	217	31	16.0	115	48	11.3	339	57
Euclidean mean	27.4	223	17	16.3	118	41	13.0	330	45

considered in the original paper, and thus will also not be discussed in the current analyses.

Two groups of in situ stress results were obtained in this area by Martin and Christiansson (1991a) based on one set of strain measurements being subjected to two interpretive models. Initially, the stress results were interpreted from strain measurements using a continuous homogeneous isotropic linear elasticity model (referred to as the "isotropic model" hereafter). This first group of stress results was tabulated in Table A1 in Martin and Christiansson (1991a). Based on these initially interpreted stress data, the 240 Level was divided into two domains (Fig. 2), i.e. a domain containing the fracture zone which has a σ_1 trend of NE–SW and a domain away from the fracture zone in which σ_1 trends approximately E–W (Martin and Christiansson 1991a). The E–W trend for σ_1 in the latter domain disagrees with the general in situ stress state around the URL, which is NE–SW and almost parallel to the Room 209 Fracture (Martin and Christiansson 1991a).

Laboratory testing of the overcore samples from boreholes in the domain away from the fracture zone showed great stress-induced micro-cracking, which created anisotropy in the overcore samples. By approximating this as transverse isotropy, the transverse plane and the anisotropic elastic constants were determined and the in situ stresses reinterpreted using an anisotropic solution based on the work of Amadei (1983, 1984) (referred to as the "anisotropic model" hereafter). This second group of stress results was shown in Table A2 in Martin and Christiansson (1991a), and—according to the original authors—is more uniform and displays better consistency with the general in situ stress state around the URL than that of the first group.

In the analysis presented here, first the scalar/vector and Euclidean means corresponding to these two interpretive models are calculated to examine the difference between the calculation approaches. Then the effective variances corresponding to these two models are obtained to confirm the authors' statements regarding the appropriateness of the anisotropic model for stress data interpretation. Finally, using the second stress data group corresponding to the anisotropic model, the influence of the fracture zone on stresses in the two domains based on proximity to the fracture zone is analysed by comparing the effective variances of the stresses in these two domains. Since in the second stress data group, the stress in borehole OC4 at the depth of 2.15 m is missing, for reasonable comparison of these two interpretive models, only 100 in situ stresses in each group are considered in the following calculations.

Table 3 Angles between the scalar/vector mean principal stress orientations of the stress data interpreted using both the isotropic and anisotropic models

Customary mean principal stresses	σ_1 and σ_2 (°)	σ_2 and σ_3 (°)	σ_3 and σ_1 (°)
Isotropic model	77	52	82
Anisotropic model	75	69	79

3 Calculation of Euclidean Mean and Its Comparison with Scalar/Vector Mean

Although Martin and Christiansson (1991a) pointed out that the scalar/vector approach may produce non-orthogonal mean principal stresses and they essentially calculated the mean stress using the correct tensorial approach, here, to compare the difference between the scalar/vector and Euclidean means and to draw people's attention regarding the error that may be caused by the scalar/vector approach, these two means of all in situ stresses interpreted using both the

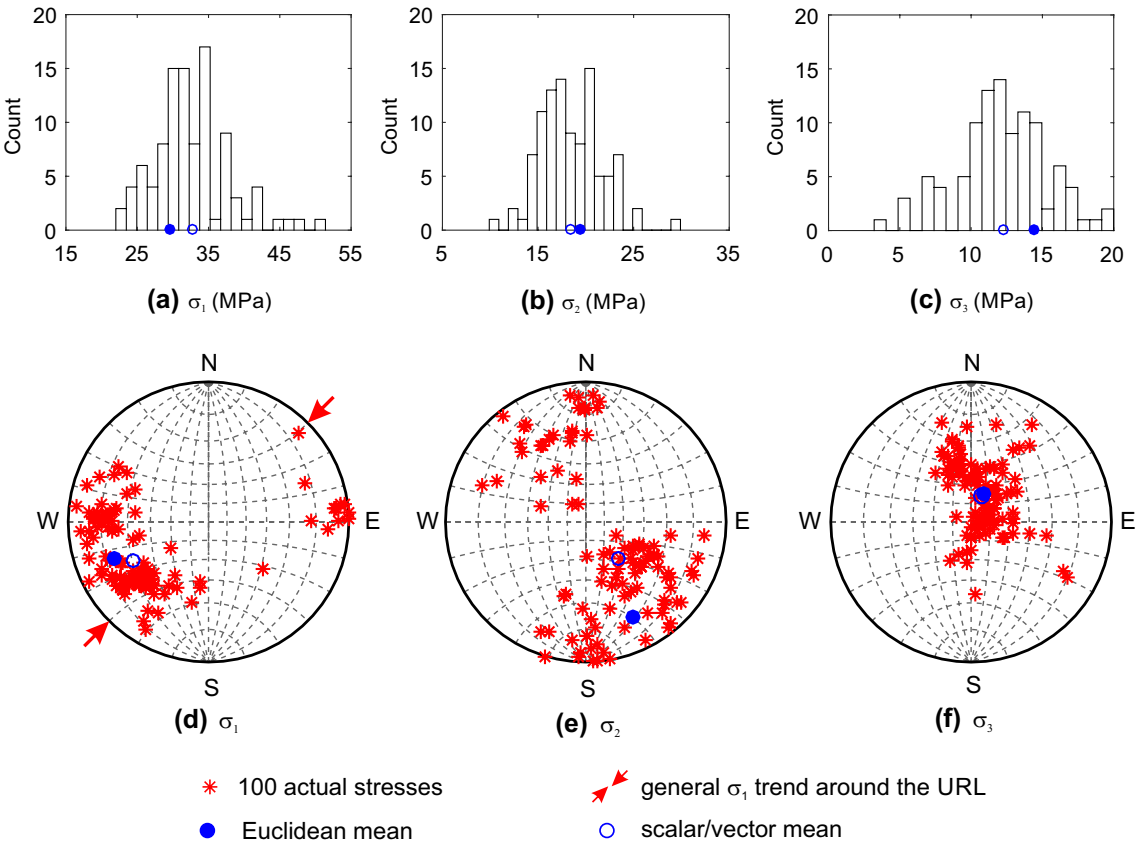

Fig. 3 Histograms of the principal stress magnitude and hemispherical projections of principal stress orientation of the in situ stress data on the 240 Level of the AECL's URL reinterpreted using the isotropic model, together with their scalar/vector mean and Euclidean mean

isotropic and anisotropic models are calculated. Particularly, to facilitate the comparison, for the Euclidean mean, after obtaining the mean stress tensor using Eq. (2), its eigenvalues and eigenvectors are further calculated to interpret the magnitudes and orientations of the principal mean stresses.

The calculated mean stresses in terms of principal stress magnitude and orientation for the isotropic and anisotropic models are tabulated in Tables 1 and 2, respectively. It can be observed that there is a distinct difference between the scalar/vector mean and Euclidean mean for both interpretative models. For example, Table 1 shows a significantly larger σ_2 plunge for the scalar/vector mean than that for the Euclidean mean, and a similar situation occurs for σ_1 plunge in Table 2. In addition, in terms of mean principal stress magnitude, the scalar/vector approach produces larger σ_1 and smaller σ_3 than the Euclidean mean; for mean principal stress orientation, the scalar/vector approach produces non-orthogonal results, as demonstrated in Table 3 by the angles between the scalar/vector mean principal stress orientations for both interpretive models.

For better comparison between the scalar/vector mean and Euclidean mean, the calculated mean stresses corresponding to each interpretive model are further plotted in Figs. 3 and 4, together with the histograms of principal stress magnitudes and hemispherical projections of principal stress orientations for each principal stress. These two figures clearly show the discrepancy in terms of both principal stress magnitude and orientation between the scalar/vector mean and the Euclidean mean. At first sight, it seems that the scalar/vector approach yields more reasonable results since both the scalar/vector mean principal stress magnitudes and orientations are located at almost the centre of their respective sample data. However, this is an artefact as the scalar/vector approach averages the principal stress magnitude and orientation separately, with the result that it yields extreme results, i.e. larger major and smaller minor principal stress magnitudes than that of the Euclidean mean. This may be because in the scalar/vector approach the principal stress magnitudes are sorted first to distinguish the major, intermediate and minor principal stresses, and then they are averaged separately. Thus, extreme results can be easily produced.

Additionally, it can be seen from Tables 1 and 2 and Figs. 3 and 4 that the σ_1 trend of the Euclidean mean of

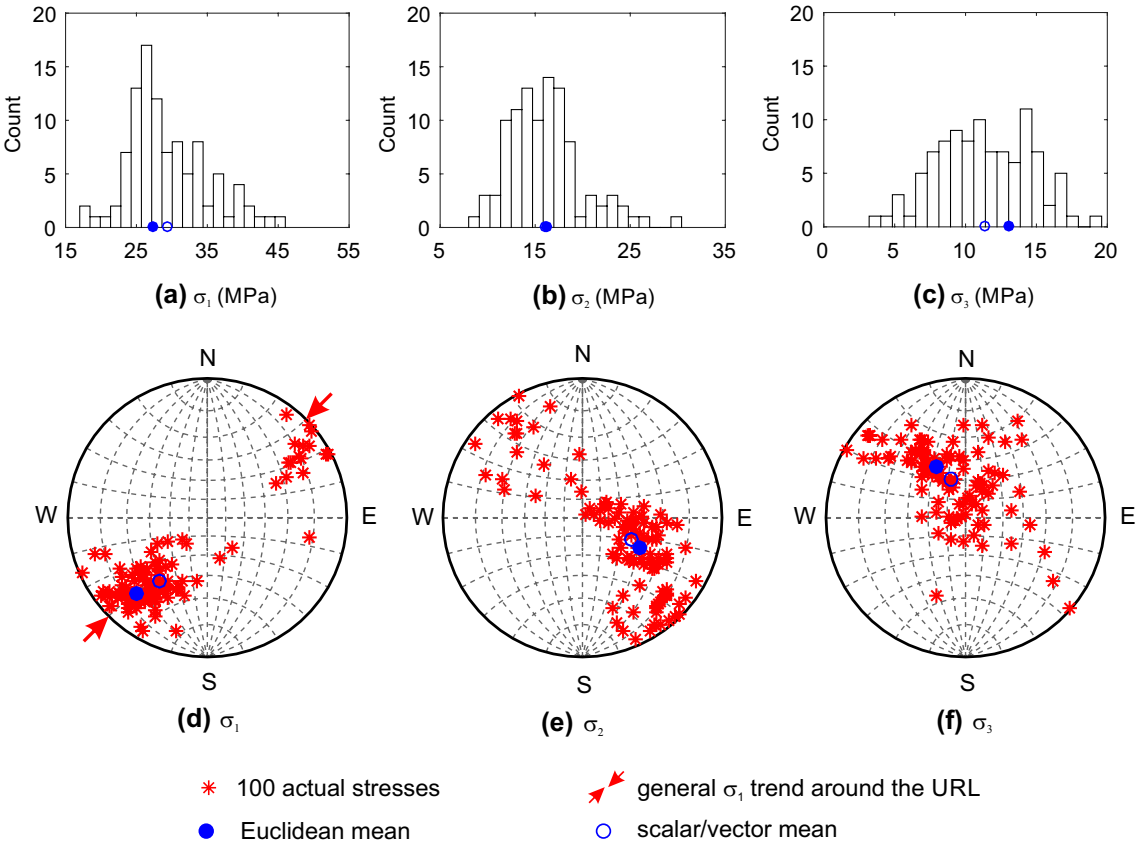

Fig. 4 Histograms of the principal stress magnitude and hemispherical projections of principal stress orientation of the in situ stress data on the 240 Level of the AECL's URL interpreted using the anisotropic model, together with their scalar/vector mean and Euclidean mean

the overall stress data reinterpreted using the anisotropic model is closer to the general in situ stress state around the URL—NE–SW, which confirms the authors' statement that the anisotropic model produces stress results more consistent with the general stress state. However, for each borehole, Martin and Christiansson (1991a) only plotted mean σ_1 trends using the stress data interpreted by the isotropic model; here, to further examine the effect of the anisotropic model on the consistency of in situ stresses with respect to the general stress state, the σ_1 trends of the Euclidean mean of the stress data from each borehole reinterpreted using the anisotropic model are also plotted (Fig. 5). The results show that, for each borehole, the mean σ_1 trends of the stress data reinterpreted using the anisotropic model are closer to the general stress state around the URL than that of the isotropic model, which is consistent with the results calculated using all stress data.

Next, stress dispersions corresponding to the two interpretive models are calculated to compare the effectiveness of the models for in situ stress measurement interpretation in terms of stress uniformity, as well as to demonstrate the efficacy of effective variance as a quantification tool for assisting in stress measurement elucidation.

4 Calculation of Stress Dispersion

Figure 5 shows that the anisotropic model generates less variable in situ stress measurement results than does the isotropic model. Here, the dispersions of the two groups of stress data interpreted using the isotropic and anisotropic models are calculated using the effective variance defined in Eq. (11). The calculated results are shown in Table 4, and show a smaller effective variance for the stress data reinterpreted using the anisotropic model than when using the isotropic model. These calculated stress dispersions provide a quantitative support to the statement in Martin and Christiansson (1991a) that by employing the anisotropic model, the interpreted stress data give a reasonably more uniform stress state on the 240 Level.

In addition, Martin and Christiansson (1991a) also asserted that the stresses in the domain containing the fracture zone are perturbed by the fracture and thus may be less uniform than the ones in the domain away from the fracture zone. To investigate this assertion, two stress domains—one containing the fracture zone (i.e. stress data from boreholes ORT1, ORT2, ORT3, OC3, OC4 and RM209) and one away from the fracture zone (stress data from boreholes OC1, OC2, OC5 and PH3)—are

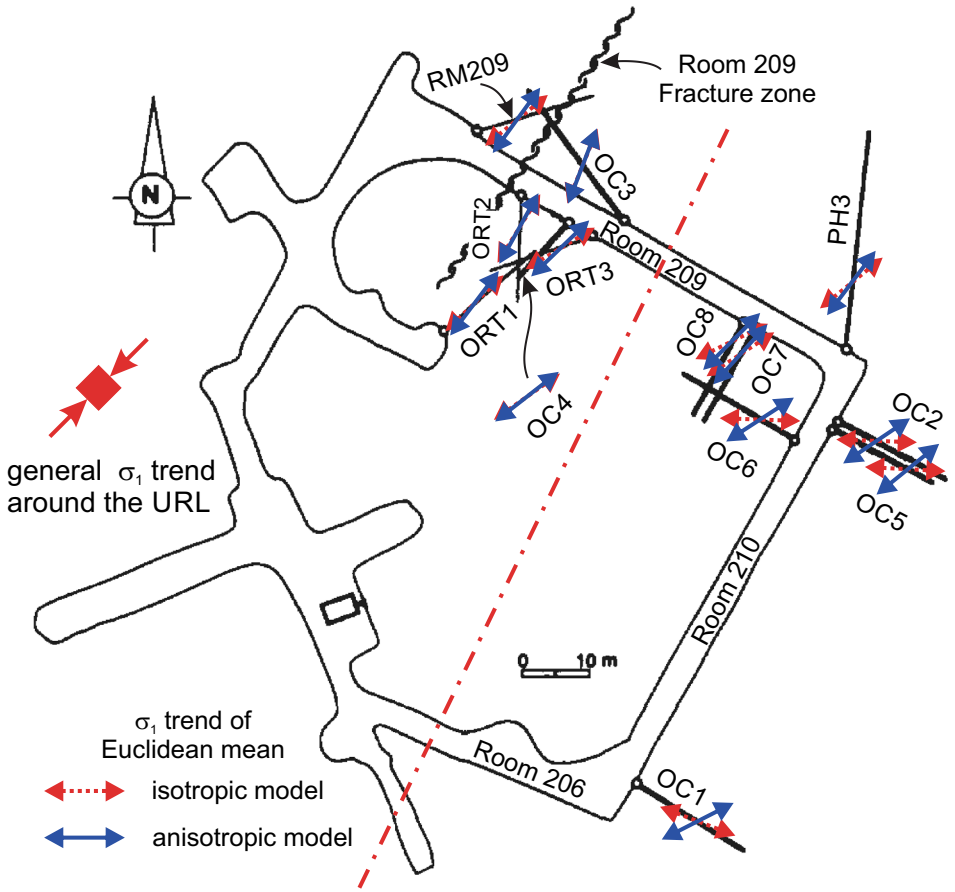

Fig. 5 Trend of major principal stress of Euclidean mean of the stress data in each borehole interpreted using the isotropic and anisotropic models (after Martin and Christiansson 1991a)

Table 4 Effective variance of the stresses interpreted using the isotropic and anisotropic models

	Isotropic model	Anisotropic model
Effective variance (MPa^2)	12.37	10.89

Table 5 Effective variances of the stress domains containing the fracture zone and away from the fracture zone using the data reinterpreted using the anisotropic model

	Domain containing fracture zone	Domain away from fracture zone
Effective variance (MPa^2)	7.69	6.78

established and their dispersions calculated to compare the influence of the fracture zone on stress variability in these two domains. To give a more distinct comparison, the stress data from boreholes OC6, OC7 and OC8 are not considered in the latter domain since they are located relatively closer to the fracture zone and Martin and Christiansson (1991a) also noted that the stress states in these three boreholes may be affected by the junction of Room 209 and Room 210. The calculated effective variances of these two domains using the data reinterpreted from the anisotropic model are shown in Table 5. The results show that the domain away from the fracture zone indeed has smaller stress dispersion and thus the stresses are more uniform and less perturbed by the fracture zone, which confirms the original authors' statement regarding the influence of the fracture zone on stress variability in a quantitative manner. Here, the relatively smaller effective variances than the effective variance of all stress data reinterpreted using the anisotropic model shown in Table 4 indicate that the stresses in each of these two individual domains are less variable when compared with the overall stress data on the 240 Level of the URL.

5 Conclusions

This paper presents an application of the proposed tensor-based mean stress and stress dispersion calculation approaches using the in situ stress data measured on the 240 Level of the AECL's URL and interpreted using both the isotropic and anisotropic models. Comparison of the scalar/vector and Euclidean mean stresses shows that the former may deviate significantly from the correct Euclidean mean, as well as producing non-orthogonal principal directions. This again confirms the drawback of the scalar/vector approach which processes principal stress magnitude and orientation separately. Calculation of the

Euclidean means of all stress data and the stress data from each borehole, interpreted using both the isotropic and anisotropic models, demonstrates that the stress data reinterpreted using the anisotropic model are closer to and consistent with the overall NE–SW orientation around the URL. Further comparison of the stress dispersion values corresponding to the two interpretative models shows that the stress states resulting from the anisotropic model show reduced dispersion than those corresponding to the isotropic model. All these quantitative calculations and comparisons confirm that approximating the rock as a transversely isotropic material due to the micro-cracking and thus using the anisotropic model for interpreting the stress at the 240 Level of the URL in Martin and Christiansson (1991a) are fulfilled. Comparison of the stress data in domains containing the fracture zone and away from the fracture zone in terms of effective variance shows that the stress state is less variable in the domain away from the fracture zone. Together, these examinations demonstrate the applicability of the proposed tensor-based stress variability characterisation approaches as effective tools to provide more detailed and quantitative elucidation of stress measurement data. All these provide, for the first time, a quantitative support to the original authors' qualitative assessments.

This paper re-examines the in situ stress data measured and interpreted almost 30 years ago. It is worth mentioning that the rock stress estimation approaches have been significantly developed in recently years, especially with the set of papers in the ISRM Suggested Methods for rock stress estimation (e.g. Christiansson and Hudson 2003; Hudson et al. 2003; Sjöberg et al. 2003; Stephansson and Zang 2012). The analyses in Martin and Christiansson (1991a), as well as in the current paper, give an indication that a stress measuring strategy with measurements in different orientations and, if possible, using alternative approaches such as considering the rock mass anisotropic properties for stress interpretation, is recommended to reduce the uncertainties related to the estimation of rock stresses.

Acknowledgements The support of the NSERC (Canada) Discovery Grant (no. 491006) and the University of Toronto are acknowledged.

Appendix A: List of Symbols

AECL	Atomic Energy of Canada Limited
URL	Underground Research Laboratory
p	Dimension of the stress tensor, $p = 2$ or 3
$\mathbf{S}_i$	ith stress tensor, $i = 1, 2, \ldots n$
$\overline{\mathbf{S}}_{\mathrm{E}}$	Euclidean mean stress tensor
$\mathbf{s}_{\mathrm{d}}$	Distinct tensor components of stress tensor $\mathbf{S}_i$
$\overline{\mathbf{s}}_{\mathrm{d}}$	Mean of $\mathbf{s}_{\mathrm{d}}$
φ	Plunge of principal stress
$\overline{\varphi}$	Mean of φ
θ	Trend of principal stress
$\overline{\theta}$	Mean of θ
σ	Normal component of stress tensor
$\overline{\sigma}$	Mean of σ
σ_1	Major principal stress
$\overline{\sigma}_1$	Mean of σ_1
σ_2	Intermediate principal stress
$\overline{\sigma}_2$	Mean of σ_2
σ_3	Minor principal stress
$\overline{\sigma}_3$	Mean of σ_3
τ	Shear component of stress tensor
$\overline{\tau}$	Mean of τ
$\mathbf{\Omega}$	Covariance matrix of distinct tensor components
$\mathrm{cov}(\cdot)$	Covariance matrix function
$V_{\mathrm{e\|d}}$	Effective variance
$\mathrm{vech}(\cdot)$	Half-vectorisation function
$\lvert \cdot \rvert$	Matrix determinant
$[\cdot]^T$	Matrix transpose

Appendix B: Euclidean Mean and Scalar/Vector Mean

Mean stress is a fundamental statistical characteristic of a stress data group and is commonly used as an indicator of the overall stress state in a rock mass (Hakala et al. 2014; Han et al. 2016; Martin 2007; Martin et al. 2003; Martin and Simmons 1993; Siren et al. 2015). Gao and Harrison (2016b) have given a rigorous derivation of how the mean stress can be calculated in a tensorial manner—the so-called Euclidean mean—based on the distance measure between stress tensors in Euclidean space. For example, when the ith stress tensor $\mathbf{S}_i$ is denoted by:

$$\mathbf{S}_i = \begin{bmatrix} \sigma_{x_i} & \tau_{xy_i} & \tau_{xz_i} \\ & \sigma_{y_i} & \tau_{yz_i} \\ \text{symmetric} & & \sigma_{z_i} \end{bmatrix}, \tag{1}$$

where σ and τ are the normal and shear tensor components, respectively, the Euclidean mean stress is given as the average of each tensor component, i.e.

$$\overline{\mathbf{S}}_{\mathrm{E}} = \frac{1}{n}\sum_{i=1}^{n}\mathbf{S}_i = \begin{bmatrix} \overline{\sigma}_x & \overline{\tau}_{xy} & \overline{\tau}_{xz} \\ & \overline{\sigma}_y & \overline{\tau}_{yx} \\ \text{symmetric} & & \overline{\sigma}_z \end{bmatrix} = \frac{1}{n}\begin{bmatrix} \sum_{i=1}^{n}\sigma_{x_i} & \sum_{i=1}^{n}\tau_{xy_i} & \sum_{i=1}^{n}\tau_{xz_i} \\ & \sum_{i=1}^{n}\sigma_{y_i} & \sum_{i=1}^{n}\tau_{yz_i} \\ \text{symmetric} & & \sum_{i=1}^{n}\sigma_{z_i} \end{bmatrix}. \tag{2}$$

Here, $\overline{\mathbf{S}}_{\mathrm{E}}$ denotes the Euclidean mean stress tensor, and $\overline{\sigma}$ and $\overline{\tau}$ denote the corresponding mean tensor components. The derivation of Euclidean mean essentially provides a theoretical support to the existing tensorial applications of calculating mean stress by averaging the corresponding stress tensor components (e.g. Dyke et al. 1987; Hudson and Cooling 1988; Koptev et al. 2013; Martin and Christiansson 1991a; Walker et al. 1990).

For the scalar/vector mean, the mean principal stress magnitudes are calculated by averaging each principal stress separately, i.e.

$$\overline{\sigma}_1 = \frac{1}{n}\sum_{i=1}^{n}\sigma_{1_i}, \quad \overline{\sigma}_2 = \frac{1}{n}\sum_{i=1}^{n}\sigma_{2_i}, \quad \overline{\sigma}_3 = \frac{1}{n}\sum_{i=1}^{n}\sigma_{3_i}, \tag{3}$$

and the principal stress orientations are calculated using directional statistics (Davis 1986, p. 333). For this, orientations are converted to unit vectors, namely,

$$x_i = \cos(\varphi_i)\cdot\sin(\theta_i+\pi), \quad y_i = \cos(\varphi_i)\cdot\cos(\theta_i+\pi), \quad z_i = \sin(\varphi_i), \tag{4}$$

where the coordinate system is x east, y north and z vertically upwards, and $\theta \in [0,\ 2\pi]$ (clockwise positive from north, looking downwards) and $\varphi \in [0,\ \pi/2]$ (positive from horizontal plane to vertically upwards) denote the trend and plunge of principal stress, respectively. The range used here for plunge avoids ambiguous results caused by the bi-directional nature of principal stress orientation. The mean vector that denotes the mean orientation is:

$$\bar{x} = \sum_{i=1}^{n}x_i \Big/ L, \quad \bar{y} = \sum_{i=1}^{n}y_i \Big/ L, \quad \bar{z} = \sum_{i=1}^{n}z_i \Big/ L, \tag{5}$$

where

$$L = \sqrt{\left(\sum\nolimits_{i=1}^{n}x_i\right)^2 + \left(\sum\nolimits_{i=1}^{n}y_i\right)^2 + \left(\sum\nolimits_{i=1}^{n}z_i\right)^2}. \tag{6}$$

The orientation of the scalar/vector mean principal stress is then

$$\begin{cases} \overline{\theta} = \begin{cases} \tan^{-1}(\bar{x}/\bar{y}) + \pi, & \text{if} \quad \bar{y} > 0 \\ \mathrm{mod}(\tan^{-1}(\bar{x}/\bar{y}), 2\pi), & \text{if} \quad \bar{y} \leqslant 0. \end{cases} \\ \overline{\varphi} = \sin^{-1}(\bar{z}) \end{cases} \tag{7}$$

Appendix C: Effective Variance—Scalar-Valued Measure of Stress Dispersion

Stress in rock often displays significant variability, and it is important that the overall variability of stress can be characterised in a quantitative manner (Gao and Harrison 2016a, 2017, 2018c; Gao and Lei 2018; Lei and Gao 2018). Dispersion, which denotes how scatter or spread out a data group is, is an effective parameter for such characterisation. Since it has been demonstrated that the variability of stress tensors can be adequately represented by the variability of its distinct tensor components in a multivariate statistics manner (Gao and Harrison 2018b), we have proposed using the widely used concept of "effective variance" in multivariate statistics for group dispersion measure (Peña and Rodríguez 2003) as a scalar-valued measure of the overall stress variability (Gao and Harrison 2016a, 2018c; Gao and Lei 2018; Lei and Gao 2018).

The effective variance of stress tensors can be calculated based on the covariance matrix of their distinct tensor components referred to a common Cartesian coordinate system. For a stress tensor denoted in Eq. (1), its distinct tensor components are:

$$\begin{aligned} \mathbf{s}_{\mathrm{d}} = \mathrm{vech}(\mathbf{S}) &= \begin{bmatrix} \sigma_x & \tau_{yx} & \tau_{zx} & \sigma_y & \tau_{zy} & \sigma_z \end{bmatrix}^T \\ &= \begin{bmatrix} \sigma_x & \tau_{xy} & \tau_{xz} & \sigma_y & \tau_{yz} & \sigma_z \end{bmatrix}^T. \end{aligned} \tag{8}$$

Here, the subscript "d" denotes "distinct", $[\,\cdot\,]^T$ represents the matrix transpose, and vech$(\cdot)$ is the half-vectorisation function which stacks only the lower triangular (i.e. on and below the diagonal) columns of a tensor into the column vector containing only its distinct components (Seber 2007, p. 246). For the stress vector $\mathbf{s}_{\mathrm{d}}$, its covariance matrix is

$$\mathbf{\Omega} = \mathrm{cov}(\mathbf{s}_{\mathrm{d}}) = \frac{1}{n}\sum_{i=1}^{n}(\mathbf{s}_{\mathrm{d}_i} - \bar{\mathbf{s}}_{\mathrm{d}})\cdot(\mathbf{s}_{\mathrm{d}_i} - \bar{\mathbf{s}}_{\mathrm{d}})^T, \tag{9}$$

where $\bar{\mathbf{s}}_{\mathrm{d}}$ denotes the mean vector and can be calculated by

$$\bar{\mathbf{s}}_{\mathrm{d}} = \frac{1}{n}\sum_{i=1}^{n}\mathbf{s}_{\mathrm{d}_i}. \tag{10}$$

Based on the covariance matrix $\mathbf{\Omega}$ given in Eq. (9), the effective variance is defined as:

$$V_{\mathrm{e|d}} = \sqrt[\frac{1}{2}p(p+1)]{|\mathbf{\Omega}|}, \tag{11}$$

where $|\cdot|$ denotes the matrix determinant and p ($p=2$ or 3) is the dimension of the stress tensor. Similar to the variance and standard deviation of scalar data, the smaller the effective variance, the more uniform would be the stress data.

References

Amadei B (1983) Rock anisotropy and the theory of stress measurements. Springer, Berlin

Amadei B (1984) In situ stress measurements in anisotropic rock. Int J Rock Mech Min Sci Geomech Abstr 21(6):327–338

Brown ET, Hoek E (1978) Trends in relationships between measured in-situ stresses and depth. Int J Rock Mech Min Sci Geomech Abstr 15(4):211–215

Chandler NA (2003) Twenty years of underground research at Canada's URL. In: WM'03 conference, Tucson, USA

Christiansson R, Hudson JA (2003) ISRM suggested methods for rock stress estimation—part 4: quality control of rock stress estimation. Int J Rock Mech Min Sci 40(7):1021–1025

Davis JC (1986) Statistics and data analysis in geology, 2nd edn. Wiley, New York

Day-Lewis AD (2008) Characterization and modeling of in situ stress heterogeneity. Ph.D. Thesis, Stanford University, California, USA

Dyke CG, Hyett AJ, Hudson JA (1987) A preliminary assessment of correct reduction of field measurement data: scalars, vectors and tensors. In: Sakurai S (ed) Proceedings of 2nd international symposium on field measurements in Geomech, Kobe, Japan. Balkema. pp 1085–1095

Dzik EJ, Walker JR, Martin CD (1989) A computer program (COSTUM) to calculate confidence intervals for in situ stress measurements, vol 1. Atomic Energy of Canada Ltd. Limited Report AECL-9575, Canada

Gao K (2017) Contributions to tensor-based stress variability characterisation in rock mechanics. Ph.D. Thesis, University of Toronto, Canada

Gao K, Harrison JP (2016a) Characterising stress dispersion for stress variability analysis. In: Johansson E (ed) RS2016 symposium—7th international symposium on in-situ rock stress, Tampere, Finland. International Society for Rock Mechanics

Gao K, Harrison JP (2016b) Mean and dispersion of stress tensors using Euclidean and Riemannian approaches. Int J Rock Mech Min Sci 85:165–173. https://doi.org/10.1016/j.ijrmms.2016.03.019

Gao K, Harrison JP (2017) Generation of random stress tensors. Int J Rock Mech Min Sci 94:18–26. https://doi.org/10.1016/j.ijrmms.2016.12.011

Gao K, Harrison JP (2018a) Examination of mean stress calculation approaches in rock mechanics. Rock Mech Rock Eng **(under review)**

Gao K, Harrison JP (2018b) Multivariate distribution model for stress variability characterisation. Int J Rock Mech Min Sci 102:144–154. https://doi.org/10.1016/j.ijrmms.2018.01.004

Gao K, Harrison JP (2018c) Scalar-valued measures of stress dispersion. Int J Rock Mech Min Sci 106:234–242. https://doi.org/10.1016/j.ijrmms.2018.04.008

Gao K, Lei Q (2018) Influence of boundary constraints on stress heterogeneity modelling. Comput Geotech 99:130–136. https://doi.org/10.1016/j.compgeo.2018.03.003

Hakala M, Ström J, Nujiten G, Uotinen L, Siren T, Suikkanen J, Oy P (2014) Thermally induced rock stress increment and rock reinforcement response, Working Report 2014-32. Posiva Oy, Helsinki, Finland

Hakami E (2011) Rock stress orientation measurements using induced thermal spalling in slim boreholes, R-11-12. SKB, Helsinki, Finland

Han J, Zhang H, Liang B, Rong H, Lan T, Liu Y, Ren T (2016) Influence of large syncline on in situ stress field: a case study of the Kaiping Coalfield, China. Rock Mech Rock Eng. https://doi.org/10.1007/s00603-016-1039-4

Hast N (1969) The state of stress in the upper part of the earth's crust. Tectonophysics 8(3):169–211

Herget G (1988) Stresses in rock. Balkema, Rotterdam

Hudson JA, Cooling CM (1988) In situ rock stresses and their measurement in the U.K.—Part I. The current state of knowledge. Int J Rock Mech Min Sci Geomech Abstr 25(6):363–370

Hudson JA, Harrison JP (1997) Engineering rock mechanics—an introduction to the principles. Elsevier, Oxford

Hudson JA, Cornet FH, Christiansson R (2003) ISRM suggested methods for rock stress estimation—Part 1: strategy for rock stress estimation. Int J Rock Mech Min Sci 40(7):991–998

Hyett AJ (1990) Numerical and experimental modelling of the potential state of stress in a naturally fractured rock mass. Ph.D., University of London, London, UK

Hyett AJ, Dyke CG, Hudson JA (1986) A critical examination of basic concepts associated with the existence and measurement of in situ stress. In: Stephansson O (ed) ISRM international symposium on rock stress and rock stress measurements, Stockholm, Sweden. International Society for Rock Mechanics, pp 387–396

Jupe AJ (1994) Confidence intervals for in situ stress measurements. Int J Rock Mech Min Sci Geomech Abstr 31(6):743–747. https://doi.org/10.1016/0148-9062(94)90013-2

Koptev AI, Ershov AV, Malovichko EA (2013) The stress state of the Earth's lithosphere: results of statistical processing of the world stress-map data. Moscow Univ Geol Bull 68(1):17–25

Lei Q, Gao K (2018) Correlation between fracture network properties and stress variability in geological media. Geophys Res Lett. https://doi.org/10.1002/2018GL077548

Lisle RJ (1989) The statistical analysis of orthogonal orientation data. J Geol 97(3):360–364

Martin CD (1990) Characterizing in situ stress domains at the AECL underground research laboratory. Can Geotech J 27(5):631–646

Martin CD (2007) Quantifying in situ stress magnitudes and orientations for Forsmark: Forsmark stage 2.2, R-07-26. SKB, Sweden

Martin CD, Christiansson RC (1991a) Overcoring in highly stressed granite—the influence of microcracking. Int J Rock Mech Min Sci Geomech Abstr 28(1):53–70

Martin CD, Christiansson RC (1991b) Overcoring in highly stressed granite: comparison of USBM and modified CSIR devices. Rock Mech Rock Eng 24(4):207–235

Martin CD, Simmons GR (1993) The Atomic Energy of Canada Limited Underground Research Laboratory: an overview of geomechanics characterization. In: Hudson JA (ed) Comprehensive rock engineering, vol 3. vol 3. Pergamon Press, Oxford, pp 915–950

Martin CD, Read RS, Lang PA (1990) Seven years of in situ stress measurements at the URL an overview. In: Hustrulid W, Johnson G (eds) 31th US symposium on rock mechanics, Golden, USA. American Rock Mechanics Association

Martin CD, Kaiser PK, Christiansson RC (2003) Stress, instability and design of underground excavations. Int J Rock Mech Min Sci 40(7–8):1027–1047

Matsumoto S, Katao H, Iio Y (2015) Determining changes in the state of stress associated with an earthquake via combined focal mechanism and moment tensor analysis: application to the 2013 Awaji Island earthquake, Japan. Tectonophysics 649:58–67

Obara Y, Sugawara K (2003) Updating the use of the CCBO cell in Japan: overcoring case studies. Int J Rock Mech Min Sci 40(7–8):1189–1203

Peña D, Rodríguez J (2003) Descriptive measures of multivariate scatter and linear dependence. J Multivar Anal 85(2):361–374

Seber GA (2007) A matrix handbook for statisticians, vol 15. Wiley, New York

Siren T, Hakala M, Valli J, Kantia P, Hudson JA, Johansson E (2015) In situ strength and failure mechanisms of migmatitic gneiss and pegmatitic granite at the nuclear waste disposal site in Olkiluoto, Western Finland. Int J Rock Mech Min Sci 79:135–148. https://doi.org/10.1016/j.ijrmms.2015.08.012

Sjöberg J, Christiansson R, Hudson JA (2003) ISRM suggested methods for rock stress estimation—Part 2: overcoring methods. Int J Rock Mech Min Sci 40(7):999–1010

Stephansson O, Zang A (2012) ISRM suggested methods for rock stress estimation—part 5: establishing a model for the in situ stress at a given site. Rock Mech Rock Eng 45(6):955–969

Walker JR, Martin CD, Dzik EJ (1990) Confidence intervals for in situ stress measurements. Int J Rock Mech Min Sci Geomech Abstr 27(2):139–141

Zhao XG, Wang J, Cai M, Ma LK, Zong ZH, Wang XY, Su R, Chen WM, Zhao HG, Chen QC, An QM, Qin XH, Ou MY, Zhao JS (2013) In-situ stress measurements and regional stress field assessment of the Beishan area. China Eng Geol 163:26–40